repiSalud
Repositorio Institucional en Salud

This is the peer reviewed version of the following article:

Rossello, X., Lopez-Ayala, P., Fernandez-Jimenez, R., Oliver, E., Galan-Arriola, C., de Molina-Iracheta, A., . . . Ibanez, B. (2020). R2 prime (R2') magnetic resonance imaging for post-myocardial infarction intramyocardial haemorrhage quantification. *European Heart Journal Cardiovascular Imaging, 21*(9), 1031-1038. doi:10.1093/ehjci/jez306

which has been published in final form at: https://doi.org/10.1093/ehjci/jez306

R2 prime (R2´) magnetic resonance imaging for post-myocardial infarction intramyocardial hemorrhage quantification

Author list:

Xavier Rossello[1,2]*, MD PhD; Pedro Lopez-Ayala[1]*, MD MSc; Rodrigo Fernández-Jiménez[1,2,3], MD PhD; Eduardo Oliver[1,2], PhD; Carlos Galán-Arriola[1,2], DVM; Antonio de Molina-Iracheta, DVM[1]; Jaume Agüero[1,2,4], MD PhD; Gonzalo J. López[1] RT; Manuel Lobo-Gonzalez[1], MD; Jean Paul Vílchez-Tschischke[1,5], MD; Valentin Fuster[1,3], MD PhD; Javier Sánchez-González[6†], PhD; and Borja Ibanez[1,2,7†], MD PhD.

[1] Centro Nacional de Investigaciones Cardiovasculares (CNIC), Madrid, Spain. [2] Centro de Investigación Biomédica en Red en Enfermedades Cardiovasculares (CIBERCV), Madrid, Spain. [3] The Zena and Michael A. Wiener Cardiovascular Institute, Icahn School of Medicine at Mount Sinai, New York, USA. [4] Cardiology Department, Hospital Universtitari i Politecnic La Fe, Valencia, Spain. [5] Complejo Hospitalario Ruber Juan Bravo, Madrid, Spain. [6] Philips Healthcare, Madrid, Spain

[7] Cardiology Department, IIS-Fundación Jiménez Díaz Hospital, Madrid.

*** Equal contribution**

† Authors for correspondence:

Borja Ibanez, MD PhD FESC. Director, Translational Laboratory for Cardiovascular Imaging and Therapy. Centro Nacional de Investigaciones Cardiovasculares Carlos III (CNIC) & IIS-Fundación Jiménez Díaz University Hospital. c/ Melchor Fernandez Almagro, 3. 28029 Madrid (Spain). Email: bibanez@cnic.es

And

Javier Sánchez-González, PhD. MR Clinical Scientist Philips Healthcare Iberia. C\ María Portugal 1, 28050 Madrid (Spain) Email: Javier.Sanchez.Gonzalez@philips.com

Abstract

Aims. To assess whether R2* is more accurate than T2* for the detection of intramyocardial hemorrhage (IMH) and to evaluate whether T2´ (or R2´) is less affected by edema than T2* (R2*), and thus more suitable for the accurate identification of post-myocardial infarction (MI) IMH.

Methods and results: Reperfused anterior myocardial infarction was performed in 20 pigs, which were sacrificed at 120 min, 24 h, 4 days, and 7 days. At each time point, cardiac magnetic resonance (CMR) T2- and T2*-mapping scans were recorded, and myocardial tissue samples were collected to quantify IMH and myocardial water content. After normalization by the number of red blood cells in remote tissue, histological IMH increased 5.2-fold, 10.7-fold, and 4.1-fold at days 1, 4 and 7, respectively. The presence of IMH was correlated more strongly with R2* (r=0.69; p=0.013) than with T2* (r=-0.50; p=0.085). The correlation with IMH was even stronger for R2´ (r=0.72; p=0.008). For myocardial edema, the correlation was stronger for R2* (r=-0.63; p=0.029) than for R2´ (r=-0.50; p=0.100). Multivariate linear regressions confirmed that R2* values were significantly explained by both IMH and edema, whereas R2´ values were mostly explained by histological IMH (p=0.024) and were little influenced by myocardial edema (p=0.262).

Conclusion: Using CMR mapping with histological validation in a pig model of reperfused MI, R2´more accurately detected IMH and was less influenced by edema than R2* (and T2*). Further studies are needed to elucidate whether R2´ is also better suited for the characterization of post-MI IMH in the clinical setting.

Keywords

Magnetic resonance imaging; intramyocardial hemorrhage; myocardial edema; myocardial infarction; myocardial reperfusion injury; myocardial inflammation

Introduction

After an acute myocardial infarction (MI), the presence and extent of intramyocardial hemorrhage (IMH) is associated with poor left ventricular (LV) remodeling[1–4] and major cardiovascular events[1,2,5,6]. There is thus a clinical need to develop an accurate method for IMH detection. Cardiac magnetic resonance (CMR) imaging allows comprehensive tissue characterization of the post-MI heart. The paramagnetic effects of deoxyhemoglobin enables myocardial iron accumulation to be detected using T2-weighted (T2W)[7–10] and T2* CMR sequences. IMH is defined as a hypointense area in the center of a hyperintense zone in edema sequences[10]. Nevertheless, although T2W CMR has been widely used to assess IMH extent[2,11–13]; T2* sequences are more accurate for IMH imaging due to their high sensitivity to the paramagnetic effects of hemoglobin breakdown[5,7,14–16].

Post-MI CMR studies dichotomizing the presence or absence of IMH use a single T2* threshold of 20 ms, based on both the ability to detect the presence of IMH (<20ms) as well its ability to confer prognostic value[5,16]. R2*, the reciprocal relaxation rate of T2* (1/T2*)[17], is well established for the quantification of liver iron concentration[18] due to its linear correlation with iron concentration[7,17]. Since T2* is the inverse of R2*, its non-transformed relationship to iron concentration is by definition non-linear[16]. This non-linear relationship could influence the interpretation of variations in T2* relaxation times in relation to iron values. Despite there is a large amount of evidence supporting the use of T2* for post-MI IMH identification and quantification[19–21], little is known regarding the use of R2* in this context and a direct comparison of T2* and R2* for the quantification of IMH (iron concentration) has not been reported yet.

Post-MI IMH co-occurs with edema, which follows a bimodal pattern[22,23]. Edema significantly changes T2-relaxation resulting in increased T2 values using cardiac relaxometry [24]. Given that T2* values are T2-dependent, the intensity of post-MI edema is predicted to impair the ability of T2* to detect IMH. A possible way to overcome the limitations of T2* for IMH detection in the presence of intense edema is to use T2 prime (T2´) values. T2´ measures the signal lost due to magnetic field inhomogeneity inside the voxel and is obtained by eliminating

T2 effects from T2* values (1/T2´=1/T2*-1/T2)[25]; T2´ should thus be less affected than T2* by the presence of post-MI edema.

The main goals of this study were 1) to determine whether R2* is more accurate than T2* for the detection of IMH across a range of IMH histological markers and 2) to evaluate whether R2´is less sensitive to edema than R2* and therefore identify more accurately the presence of post-MI IMH. For the study, we used a translatable large animal (pig) model of myocardial ischemia/reperfusion (I/R) followed by serial CMR examination and histological IMH validation.

Methods

Study design

The study population consisted of 20 Large-white male pigs weighing 30 kg to 40 kg each[22]. The study was approved by the Institutional Animal Research Committee and conducted in accordance with the recommendations of the Guide for the Care and Use of Laboratory Animals. The study design is summarized in **Figure 1**. Reperfused acute MI was induced in 20 pigs by closed-chest 40-min left anterior descending (LAD) coronary artery occlusion followed by reperfusion. Pigs were sacrificed at 4 time-points after reperfusion: 120 min, 24 h, 4 days, and 7 days (n= 5 per time point). CMR scans were performed at every follow-up stage until sacrifice (i.e., animals sacrificed on day 7 underwent CMR exams at baseline, 120 min, 24 h, day 4, and day 7). Pigs were sacrificed after the final follow-up CMR scan, and myocardial tissue samples were collected from the ischemic and remote areas for evaluation of IMH and water content. One pig from the 120 min group died immediately after the 120 min CMR scan; in this animal, CMR and water content data were available, but histological assessment was not possible due to technical problems with sample processing.

Myocardial infarction procedure

The I/R protocol has been detailed elsewhere[22]. Anesthesia was induced by intramuscular injection of ketamine (20 mg/kg), xylazine (2 mg/kg), and midazolam (0.5 mg/kg) and maintained

by continuous intravenous infusion of ketamine (2 mg/kg/h), xylazine (0.2 mg/kg/h), and midazolam (0.2 mg/kg/h). Animals were intubated and mechanically ventilated with a 28% fraction of inspired oxygen. A single bolus of 300 IU/kg unfractionated heparin was administered at the onset of instrumentation through the central venous line. The LAD coronary artery was occluded immediately distal to the origin of the first diagonal branch for 40 min with an angioplasty balloon introduced via the percutaneous femoral route using the Seldinger technique. Balloon location and maintenance of inflation were monitored angiographically. After balloon deflation, a coronary angiogram was recorded to confirm patency of the LAD. To prevent malignant ventricular arrhythmias, a continuous infusion of amiodarone (300 mg/h) was initiated at the time of balloon occlusion (no bolus) and maintained throughout the procedure in all pigs. In cases of ventricular fibrillation, non-synchronized shocks were delivered using a biphasic defibrillator.

CMR protocol

All studies were performed in a Philips 3-T Achieva Tx whole-body scanner (Philips Healthcare, Best, the Netherlands) equipped with a 32-element phased-array cardiac coil. Among other sequences, the imaging protocol included a standard segmented cine steady-state free-precession (SSFP) sequence to provide high-quality anatomical references, as well as T2 and T2* mapping sequences using multi-echo gradient spin echo sequence (GraSE). The imaging parameters for the SSFP sequence were field of view (FOV), 280x280 mm^2; slice thickness, 6mm with no gaps; repetition time (TR), 2.8 ms; echo time (TE), 1.4 ms; flip angle, 45^o; cardiac phases, 30 (temporal resolution of 33ms for a heart rate of 60 bpm); voxel size, 1.8x1.8 mm^2; and number of excitations (NEX), 3. The imaging parameters for the T2-GraSE mapping sequence were FOV, 300x300 mm^2; slice thickness, 8 mm; TR, 2 heartbeats; and 8 echo times ranging from 6.5 to 52.0 ms. T2 mapping had an in-plane resolution of 1.8x2.0 mm^2 in AP and LR directions, respectively with a slice thickness of 8 mm. Phase encoding direction was defined in the LR direction with a SENSE factor of 2. The T2* mapping sequence had the same FOV and resolution as used for T2 mapping. Eight echoes were acquired, ranging from 2.2 to 21.1 ms. A flip angle of 15^o was used

to ensure a balance between a high signal-to-noise ratio and T1 effects. The same imaging protocol was used at every time points.

Cardiovascular magnetic resonance analysis

CMR images were analyzed using dedicated software (MR Extended Work Space 2.6, Philips Healthcare, and QMass MR 7.6, Medis, Leiden, the Netherlands) by 2 experienced CMR analysts blinded to the pathology results., T2*, R2 and R2* maps were automatically generated in the acquisition scanner by fitting the signal intensity of all echo times at each pixel to a monoexponential decay curve using a maximum likelihood expectation maximization algorithm. IMH was defined on T2* images as an hypointense core within the infarct hyperintense area, and then confirmed in R2 and R2* maps. T2*, R2 and R2* relaxation maps were quantitatively analyzed by drawing a region of interest (ROI) around the hypointense infarct core of the corresponding mid-ventricular section in all T2* (and R2*) images and copying this ROI onto the corresponding R2 maps (**Figure 2**). When no hypointense infarct core was observed, a ROI was drawn in the middle of the wall of the left ventricle on T2* and R2 maps, never surpassing the ischemic region assessed by the extent of edema. R2´ values were calculated from R2 and R2* values. All values were calculated as means.

Histopathological analysis

A detailed description of the Histopathological analysis is described in Supplemental material. Paired myocardial samples were collected in all pigs within minutes of euthanasia from the infarcted core and the remote myocardium. IMH was defined as the presence of extravasated red blood cells (RBCs) within the interstitium between cardiomyocytes or surrounding microvessels with a disrupted endothelial barrier within the infarcted zone[26] **(Figure 3).** Microvascular obstruction (MVO) was defined as any plug formed in a microvessel with an intact endothelium and accompanied by an accumulation of RBCs (RBCs “trapped” within vessels)[27]

(Figure 3). All histological samples were evaluated by an experienced pathologist blinded to all other data.

The focus of our histological assessment was on hemorrhagic regions, defined as any region with extravasated erythrocytes (**Figure S1**), excluding therefore regions with erythrocytes confined within a vessel with intact endothelium (defined as MVO) or located in healthy myocardium or granulation tissue (GT). RBC density per mm^2 in the infarcted core was thus calculated by dividing the area occupied by RBCs in the IMH region(s) by the total area of pathological myocardium (IMH and MVO regions). RBC per mm^2 was also calculated for the remote myocardium, as the ratio of the area occupied by RBCs to the total remote myocardium area, and used as the benchmark value. IMH was quantified for each sample pair as the fold difference between RBC/mm^2 in the infarcted region and its matched remote myocardium sample (normalized erythrocyte density, NED; the histological measure of IMH).

The quantification of myocardial water content in myocardial samples has been described previously[22,28]. Briefly, tissue water content was calculated as follows: water content (%) = ([wet weight – dry weight]/wet weight) x 100.

Histopathological heart slices were matched with CMR images by consensus of 2 experienced readers, using the posterior papillary muscle anatomical landmark and the slice position in relation to the mitral valve annulus and the apex.

Statistical analysis

The normal distribution of each data subset was evaluated using graphical methods. Continuous variables are expressed as mean ± standard deviation (SD). For comparisons among animals sacrificed at different time points, water content was compared by one-way analysis of variance. Between-group differences in histological IMH were assessed by the Kruskal-Wallis test. Associations between CMR relaxation times (T2*, R2*, and R2´) and histological IMH were evaluated with the Pearson correlation coefficient. A sensitivity analysis avoiding the assumption

of linear association between variables was performed using the Spearman rank correlation coefficient.

Univariate and multivariate linear regressions were performed to assess the association of values from each CMR sequence (R2* and R2' as dependent variables) with water content and IMH (predictor variables): model A evaluated the association with water content, model B the association with IMH, and model C the association with water content and IMH simultaneously. The magnitude of the difference across comparisons was assessed with beta coefficients (or slopes, which show the expected increase in the dependent variable per unit increase in the predictor/s) and the determination coefficient (or R^2, which is the percentage of the variability explained by the predictor/s in the dataset). p-values for these comparisons were obtained with Wald tests.

Differences were considered statistically significant at $p<0.05$. All statistical analyses were performed in STATA version 15.1 (Stata Corp, College Station, TX, USA). Some figures were produced in GraphPad Prism 6.00 (GraphPad Software, La Jolla California).

Results

Histological IMH dynamics after reperfused-myocardial infarction

Histology was used as the gold standard for IMH quantification. Samples for this analysis came from a group of animals whose water content results were previously reported[22]. Data regarding myocardial infarct size, myocardium at risk and extension of IMH has been reported elsewhere[23]. IMH was absent at 120 minutes post-reperfusion but was evident to some extent in 80% of pigs sacrificed at later time points (4/5 pigs sacrificed at 24 hours, 4/5 pigs sacrificed at 4 days, and 4/5 pigs sacrificed at 7 days). H&E staining showed large areas of RBC extravasation in the infarct core at 24 hours and at 4 and 7 days post-reperfusion. At 120 minutes, MVO was found in the center of the infarct core, whereas at 24 hours MVO was confined to the border zone (**Figure S1**). Histological IMH (measured relative to remote tissue by NED) was 5.2-fold higher

in the infarct core at 24 hours, 10.7-fold higher at day 4, and 4.1-fold higher at day 7. Histological IMH and water content results are summarized in **Figure S3**.

Correlation of T2* and R2* with IMH

To avoid artifacts in linear correlations, pigs without IMH were excluded from the evaluation of the association between CMR values and histological IMH (correlations including animals without hemorrhage are presented in **Figure S4**). Thus, correlations were performed using those 12 pigs with histological IMH. T2* showed a non-significant negative correlation with histological IMH (r=-0.50; p=0.095). Conversely, R2* and histological IMH showed a strong positive linear correlation (r=0.69; p=0.013) (**Figure 4**). These findings prompted us to focus on R2* values rather than T2*. The Spearman rank correlation coefficients were consistent with our findings (**Table S1**).

Correlation of R2* and R2´ with IMH and myocardial water content

The positive correlation with IMH was even stronger for R2´ (r=0.72; p=0.008) (**Figure 5 panel A**). Moreover, the stronger association of R2´ vs R2* with IMH was maintained when animals without IMH were included in the analysis (**Fig S5 panel A**). A moderate negative correlation was found between R2* and myocardial edema (% water content) (r=-0.63; p=0.029) (**Figure 5 panel B**). Conversely, R2´ showed a non-significant negative correlation with water content (r=-0.50; p=0.100). When animals without IMH are included in the associations, the association of R2´ with edema remained weaker than that of R2* (**Fig S5 panel B**).

Influence of myocardial edema on the ability of R2* and R2´ to accurately detect IMH

Univariate and multivariate linear regressions were performed to assess the association of each sequence (R2* and R2´) with IMH and water content (%), alone and in combination. Six

linear regression models for pigs with IMH are reported in **Table 1**; the results for all pigs (with and without IMH) are reported in **Table S2**.

In univariate analyses (models A and B), R2* showed a significant association with IMH and water content, whereas R2´ was significantly associated with IMH and showed a trend toward significance for its association with water content. However, the magnitude of association for each parameter, measured as the determination coefficient (R^2), differed between regression models. For the regression models relating water content to CMR values, R^2 was greater for R2* (water content explained 39% of R2* variations but only 25% of R2´ variations). In contrast, IMH showed a stronger association with R2´ (IMH explained 48% of R2* variations and 52% of R2´ variations).

In multivariate analyses, R2* values were significantly explained by both IMH and water content; in contrast, R2´ values were mostly explained by histological IMH (p=0.024) but showed little association with myocardial water content (p=0.262). This is also evident from the relative change of the partial regression coefficient between regressions: a reduction from 0.0032 in the univariate analysis to 0.0028 in the multivariate analysis for R2´, compared with a reduction from 0.0033 to 0.0026 for R2*, suggesting that R2´ is less influenced by myocardial water content when this parameter is considered in the model.

Discussion

Recent studies have reported that IMH is a strong predictor of poor LV remodeling[1–3] and major cardiovascular events[1,2,5]. Optimal CMR mapping sequences are needed to define the prognostic impact of IMH in post-MI patients and eventually to guide future interventions. In the present study, we used state-of-the-art CMR mapping parameters and histological validation in an *in vivo* large animal model that closely resembles human acute MI. Our results show that (i) R2* shows a closer linear correlation with IMH than its reciprocal parameter T2* and is thus a better estimator of IMH; (ii) The correlation of R2* with IMH is significantly impaired by the presence of post-MI edema; (iii) R2´ is significantly correlated with IMH and its accuracy is less

affected by post-MI edema than that of R2*. Therefore, in the post-MI setting, R2´ mapping outperforms R2* (and its inverse T2*) for the evaluation of IMH.

The degradation of hemoglobin products causes local magnetic field inhomogeneities that result in signal intensity loss on T2-weighted and T2*-weighted CMR images[29]. T2 is highly sensitive to myocardial edema, reducing the resolution for delineating the hypointense core within the infarcted region in the post-MI period (which is characterized by an intense bimodal edema reaction)[22,23]. Conversely, T2*-based CMR imaging is more sensitive to the hemorrhagic response[6]. Consequently, T2* mapping is considered the optimal technique for IMH identification and quantification[7,16], and thresholds have been proposed for the detection of IMH (eg, 20 ms in 1.5T CMR) [5,16]. The novelty of our findings lies in demonstrating that the use of the inverse transformations of T2* mapping parameters (R2* and R2´) increases the accuracy of IMH severity detection. T2* mapping parameters had been used before to objectively evaluate IMH in animal models[19,30] or in the clinic[5,9,13,19]; however, there is a paucity of published data demonstrating a potential role for R2* and R2´ in the heart[17].

In a classic study assessing the role of T2* CMR in the early diagnosis of myocardial iron overload, Anderson and colleagues described a curvilinear, inverse association between biopsy-determined iron concentration and liver T2*; log transformation of T2* yielded a negative log-linear correlation that facilitated the interpretation of the study findings[16]. In our study, we used the inverse transformation of T2* parameters (R2* from 1/T2*, and R2´ from the difference between R2* and R2 (R2*-R2)). R2* is already used clinically to assess hepatic iron content[18,31], but has barely been used in the heart[17], and there is no previously published evidence for its potential to detect IMH in post-reperfused MI. Even less is available on the use of R2´; however, some researchers have proposed that R2´ may be a more sensitive marker of tissue iron in other organs[32,33].

The influence of myocardial edema on CMR parameter values should be considered in the evaluation of post-reperfused MI tissue[6], particularly in relation to its dynamic pattern during reperfusion injury. The measured value of a T2 parameter (and also its inverse, R2) may be determined by more than one confounding factor occurring simultaneously[7], such as IMH, edema,

or an unknown underlying disease processes. We used multivariate regression to ascertain the impact of the edematous and hemorrhagic reactions on R2* and R2´ values. One of the main conclusions of our analysis is that most of the R2´ variability can be explained by the IMH component, with myocardial edema having little impact on this parameter. In contrast, R2* can be explained by both components with a similar degree of statistical significance, and the counterbalancing effects of IMH and myocardial water content therefore cannot be defined unambiguously.

Our results regarding the edema bimodal pattern and the influence of water content on T2* challenge the current use of thresholds for edema-dependent parameters, such as the detection of post-MI IMH. Previous studies using 1.5T CMR have applied a cut-off value for T2* of <20 ms to detect IMH[5,16] and cardiac iron overload[7], but a threshold-based method of 2 SD units below the mean remote myocardial T2* has also been accepted[8]. CMR visualization of IMH is possible because of the degradation of erythrocytes into breakdown products, such as oxyhemoglobin, deoxyhemoglobin, and methemoglobin, which generate distinct signal intensities on CMR and thus make IMH both time- and sequence-dependent[3]. In addition, interpretation of T2* (and R2*) results is further limited by the presence of the post-MI bimodal edematous reaction. The use of CMR parameters such as R2´, with higher sensitivity to the severity of IMH and little influence from myocardial water content, would allow noninvasive assessment of the time-course of IMH in post-MI patients, especially in the early post-MI period. Further studies are needed to establish appropriate cut-off values for R2´ for accurate quantification of IMH severity at each time-point.

In this study, R2* and R2 were estimated (and R2' computed) from separate data acquisition. Although combining T2 and T2* acquisition may be attractive to obtain all required weights to generate R2’ maps in a single acquisition, this approach also presents some limitation when it would be applied in a real clinical scenario, by limiting the number of spin echoes and/or gradient echoes TE to enable the acquisition in a single breath-hold. In addition, TFE and/or EPI factor should be limited to ensure proper sampling of gradient echo TE. To compensate this limitation higher parallel acquisition factor or compressed sensing techniques may be applied.

Study limitations

Caution is needed when extrapolating these findings to the clinical arena. The intensity and time course of IMH in post-MI patients might be modified by several factors, such as the amount of collateral flow, ischemic preconditioning, necrotic extents, distal coronary microembolization, and differences in individual risk factors such as diabetes or smoking[13]. Nonetheless, the use of a large animal model is of great translational value, particularly considering the difficulties of performing a longitudinal CMR assessment in the clinical setting and the impossibility of histopathological validation. Although the pig model of reperfusion MI closely represents the human setting, there are some differences between the incidence of IMH in our experimental data and the 25%-50% incidence reported for patients[1–3]. The pig model of ischemia/reperfusion is known to be very prone to developing IMH. This study was not designed to establish an association between the anatomical area of IMH and the extent of CMR-visualized IMH, but rather to make associations between the degree of hemorrhage (measured by NED) and CMR mapping parameters (relaxation values). Moreover, the ROI around the hypointense infarct core might include not only IMH, but also MVO. The equation presented demonstrating the relationship of R2, R2* and R2' is based on the assumption that all relaxations are monoexponential. Our regression models left a great amount of unexplained variability, which can be partly attributed to noise in the parameter estimation (particularly for R2') and the amount of erythrocytes in the extravascular space. Caution should be exercised when extrapolating results to other MI in other heart regions, although the observed histological changes are likely to occur regardless of MI location. We restricted our analysis to anterior MIs to avoid potential magnetic-field nonhomogeneities related to the interolateral wall and to adhere to recommendations for patient selection in clinical trials testing cardioprotective interventions. However, this restriction is in line with the predominance of IMH in anterior infarcts in humans[13].

Our data lacks data regarding T1 imaging, despite some studies have also investigated the ability to detect and quantify IMH using T1 CMR[10]. Nevertheless, these studies have shown

that the sensitivity to detect post-MI IMH is often compromised by the opposite effects that hemorrhage and edema impose on T1[3,10,34].

Conclusions

Using CMR mapping analyses and histological validation in a pig model of post-reperfused MI, we found that the strong ability to accurately portray the degree of IMH provided by R2´ in addition to its relative insensitivity to myocardial edema may make this technique better suited than R2* (and T2*) for the characterization of post-MI IMH. The counteracting effects of IMH and edema are less conspicuous on R2´, as demonstrated after the adjustment for IMH and myocardial water content in a set of multivariate linear regressions. Further research is needed to evaluate whether these findings can be extrapolated to the clinical setting in order to better stratify risk prognosis for poor LV remodeling and major adverse cardiovascular events and to accurately assess the impact of potential cardioprotective therapies on reperfusion-induced IMH.

Disclosures

Dr Sánchez-González is a Philips Healthcare employee. The other authors declare no conflict of interest.

Sources of Funding

This study was partially supported by a competitive grant from the Carlos III Institute of Health–Fondo de Investigacion Sanitaria and the European Regional Development Fund (ERDF/FEDER) (PI13/01979), the Spanish Ministry of Science, Innovation and Universities (MICINN) and ERDF/FEDER SAF2013-49663-EXP. This study forms part of a Master Research Agreement between the CNIC and Philips Healthcare, and is part of a bilateral research program between Hospital de Salamanca Cardiology Department and the CNIC. This research program is part of an institutional agreement between FIIS Fundación Jiménez Díaz and the CNIC. The CNIC is supported by the Ministry of Science, Innovation and Universities (MICINN), the Instituto de Salud Carlos III (ISCiii), and the Pro CNIC Foundation, and is a Severo Ochoa Center of Excellence (award SEV-2015-0505). X.R. has received support from the SEC-CNIC CARDIOJOVEN fellowship program. RF-J is a recipient of funding from the European Union Horizon 2020 research and innovation programme under the Marie Skłodowska-Curie grant agreement No. 707642.

Acknowledgements

The authors thank T. Córdoba, O. Sanz, E. Fernández, and other members of the CNIC animal facility and farm for outstanding animal care and support. S. Bartlett (CNIC) provided English editing.

References

1. Ganame J, Messalli G, Dymarkowski S, Rademakers FE, Desmet W, Van de Werf F, et al. Impact of myocardial haemorrhage on left ventricular function and remodelling in patients with reperfused acute myocardial infarction. Eur Heart J 2009;30:1440–1449.
2. Eitel I, Kubusch K, Strohm O, Desch S, Mikami Y, de Waha S, et al. Prognostic Value and Determinants of a Hypointense Infarct Core in T2-Weighted Cardiac Magnetic Resonance in Acute Reperfused ST-Elevation-Myocardial Infarction. Circ Cardiovasc Imaging 2011;4:354–362.
3. Betgem RP, Waard GA de, Nijveldt R, Beek AM, Escaned J, van Royen N. Intramyocardial haemorrhage after acute myocardial infarction. Nat Rev Cardiol 2015;12:156–167.
4. Mather AN, Fairbairn TA, Ball SG, Greenwood JP, Plein S. Reperfusion haemorrhage as determined by cardiovascular MRI is a predictor of adverse left ventricular remodelling and markers of late arrhythmic risk. Heart 2011;97:453–459.
5. O'Regan DP, Ariff B, Neuwirth C, Tan Y, Durighel G, Cook SA. Assessment of severe reperfusion injury with T2* cardiac MRI in patients with acute myocardial infarction. Heart 2010;96:1885–1891.
6. Carrick D, Haig C, Ahmed N, McEntegart M, Petrie MC, Eteiba H, et al. Myocardial Hemorrhage After Acute Reperfused ST-Segment-Elevation Myocardial Infarction: Relation to Microvascular Obstruction and Prognostic Significance. Circ Cardiovasc Imaging 2016;9:e004148.
7. Messroghli DR, Moon JC, Ferreira VM, Grosse-Wortmann L, He T, Kellman P, et al. Clinical recommendations for cardiovascular magnetic resonance mapping of T1, T2, T2* and extracellular volume: A consensus statement by the Society for Cardiovascular Magnetic Resonance (SCMR) endorsed by the European Association for Cardiovascular Imaging (EACVI). J Cardiovasc Magn Reson 2017;19:75.

8. Bulluck H, Dharmakumar R, Arai AE, Berry C, Hausenloy DJ. Cardiovascular Magnetic Resonance in Acute ST-Segment-Elevation Myocardial Infarction: Recent Advances, Controversies, and Future Directions. Circulation 2018;137:1949–1964.

9. Zia MI, Ghugre NR, Connelly KA, Strauss BH, Sparkes JD, Dick AJ, et al. Characterizing Myocardial Edema and Hemorrhage Using Quantitative T2 and T2* Mapping at Multiple Time Intervals Post ST-Segment Elevation Myocardial Infarction. Circ Cardiovasc Imaging 2012;5:566–572.

10. Ibanez B, Aletras AH, Arai AE, Arheden H, Bax J, Berry C, et al. Cardiac MRI Endpoints in Myocardial Infarction Experimental and Clinical Trials. J Am Coll Cardiol 2019;74:238–256.

11. Basso C, Corbetti F, Silva C, Abudureheman A, Lacognata C, Cacciavillani L, et al. Morphologic validation of reperfused hemorrhagic myocardial infarction by cardiovascular magnetic resonance. Am J Cardiol 2007;100:1322–1327.

12. Payne AR, Berry C, Kellman P, Anderson R, Hsu L-Y, Chen MY, et al. Bright-blood T(2)-weighted MRI has high diagnostic accuracy for myocardial hemorrhage in myocardial infarction: a preclinical validation study in swine. Circ Cardiovasc Imaging 2011;4:738–745.

13. Hamirani YS, Wong A, Kramer CM, Salerno M. Effect of Microvascular Obstruction and Intramyocardial Hemorrhage by CMR on LV Remodeling and Outcomes After Myocardial Infarction. JACC Cardiovasc Imaging 2014;7:940–952.

14. Wiesmann M, Mayer TE, Yousry I, Hamann GF, Brückmann H. Detection of hyperacute parenchymal hemorrhage of the brain using echo-planar T2*-weighted and diffusion-weighted MRI. Eur Radiol 2001;11:849–853.

15. Atlas SW, Mark AS, Grossman RI, Gomori JM. Intracranial hemorrhage: gradient-echo MR imaging at 1.5 T. Comparison with spin-echo imaging and clinical applications. Radiology 1988;168:803–807.

16. Anderson LJ, Holden S, Davis B, Prescott E, Charrier CC, Bunce NH, Firmin DN, Wonke B, Porter J, Walker JM, Pennell DJ. Cardiovascular T2-star (T2*) magnetic

resonance for the early diagnosis of myocardial iron overload. Eur Heart J 2001;22:2171–2179.

17. Carpenter J-P, He T, Kirk P, Roughton M, Anderson LJ, de Noronha SV, et al. On T2* magnetic resonance and cardiac iron. Circulation 2011;123:1519–1528.

18. Wood JC, Enriquez C, Ghugre N, Tyzka JM, Carson S, Nelson MD, et al. MRI R2 and R2* mapping accurately estimates hepatic iron concentration in transfusion-dependent thalassemia and sickle cell disease patients. Blood 2005;106:1460–1465.

19. Kali A, Tang RLQ, Kumar A, Min JK, Dharmakumar R. Detection of acute reperfusion myocardial hemorrhage with cardiac MR imaging: T2 versus T2. Radiology 2013;269:387–395.

20. Kumar A, Green JD, Sykes JM, Ephrat P, Carson JJL, Mitchell AJ, et al. Detection and quantification of myocardial reperfusion hemorrhage using T2*-weighted CMR. JACC Cardiovasc Imaging 2011;4:1274–1283.

21. Kali A, Kumar A, Cokic I, Tang RLQ, Tsaftaris SA, Friedrich MG, et al. Chronic manifestation of postreperfusion intramyocardial hemorrhage as regional iron deposition: a cardiovascular magnetic resonance study with ex vivo validation. Circ Cardiovasc Imaging 2013;6:218–228.

22. Fernández-Jiménez R, Sánchez-González J, Agüero J, García-Prieto J, López-Martín GJ, García-Ruiz JM, et al. Myocardial Edema After Ischemia/Reperfusion Is Not Stable and Follows a Bimodal Pattern. J Am Coll Cardiol 2015;65:315–323.

23. Fernández-Jiménez R, Barreiro-Pérez M, Martin-García A, Sánchez-González J, Agüero J, Galán-Arriola C, et al. Dynamic Edematous Response of the Human Heart to Myocardial Infarction: Implications for Assessing Myocardial Area at Risk and Salvage. Circulation 2017;136:1288–1300.

24. Fernández-Jiménez R, Sánchez-González J, Aguero J, del Trigo M, Galán-Arriola C, Fuster V, et al. Fast T2 gradient-spin-echo (T2-GraSE) mapping for myocardial edema quantification: first in vivo validation in a porcine model of ischemia/reperfusion. J Cardiovasc Magn Reson 2015;17:92.

25. Chavhan GB, Babyn PS, Thomas B, Shroff MM, Haacke EM. Principles, techniques, and applications of T2*-based MR imaging and its special applications. Radiographics 2009;29:1433–1449.

26. Buja LM, Butany J. Cardiovascular pathology. Boston: Elsevier 2015.

27. Driesen RB, Zalewski J, Vanden Driessche N, Vermeulen K, Bogaert J, Sipido KR, et al. Histological correlate of a cardiac magnetic resonance imaged microvascular obstruction in a porcine model of ischemia-reperfusion. Cardiovasc Pathol 2012;21:129–131.

28. Fernández-Jiménez R, García-Prieto J, Sánchez-González J, Agüero J, López-Martín GJ, Galán-Arriola C, et al. Pathophysiology Underlying the Bimodal Edema Phenomenon After Myocardial Ischemia/Reperfusion. J Am Coll Cardiol 2015;66:816–828.

29. Bradley WG. MR appearance of hemorrhage in the brain. Radiology 1993;189:15–26.

30. Ghugre NR, Ramanan V, Pop M, Yang Y, Barry J, Qiang B, et al. Quantitative tracking of edema, hemorrhage, and microvascular obstruction in subacute myocardial infarction in a porcine model by MRI. Magn Reson Med 2011;66:1129–1141.

31. St Pierre TG, Clark PR, Chua-anusorn W, Fleming AJ, Jeffrey GP, Olynyk JK, et al. Noninvasive measurement and imaging of liver iron concentrations using proton magnetic resonance. Blood 2005;105:855–861.

32. Graham JM, Paley MN, Grünewald RA, Hoggard N, Griffiths PD. Brain iron deposition in Parkinson's disease imaged using the PRIME magnetic resonance sequence. Brain 2000;123:2423–2431.

33. Miszkiel KA, Paley MN, Wilkinson ID, Hall-Craggs MA, Ordidge R, Kendall BE, et al. The measurement of R2, R2* and R2' in HIV-infected patients using the prime sequence as a measure of brain iron deposition. Magn Reson Imaging 1997;15:1113–1119.

34. Wang G, Yang H-J, Kali A, Cokic I, Tang R, Xie G, Yang Q, Francis J, Li S, Dharmakumar R. Influence of Myocardial Hemorrhage on Staging of Reperfused Myocardial Infarctions With T2 Cardiac Magnetic Resonance Imaging. JACC Cardiovasc Imaging 2019;12:693–703.

Tables

Table 1. Linear regression models developed to explain R2* and R2´ values using water content and intramyocardial hemorrhage values

		R2*			R2'		
		Coefficient for R2*	**P-value**	**R^2**	**Coefficient for R2´**	**P-value**	**R^2**
Model A	Water	-0.0101	0.029	0.39	-0.0074	0.100	0.25
Model B	IMH	0.0033	0.013	0.48	0.0032	0.008	0.52
Model C	Water	-0.0070	0.070	0.65	-0.0041	0.262	0.58
	IMH	0.0026	0.033		0.0028	0.024	

Only pigs with IMH are included in this table (table S3 shows the analogue results for all pigs). Model A and model B are univariate regressions, whereas model C is a multivariate analysis for water content and IMH.

The interpretation of the estimated partial regression coefficient for R2* in model C is that the estimated mean increase in R2* values per one unit increase in NED (the histological measure of IMH) among animals with the same water content is 0.0026 $msec^{-1}$. In other words, it is the slope of the R2* increase per unit increase of histological IMH when water content is controlled. Negative values observed for water content indicate a negative linear association (the lower the water content, the lower the values of R2* or R2´). The determination coefficient (R^2) should be understood as the percentage of the variability of R2* or R2´ explained by the predictor/s. Thus, histological IMH explains 52% of the variability in R2´ (model B), whereas water content and histological IMH together explain 58% of R2´ variability (model C). Wald tests were used to assess the statistical significance of adding predictors to the equation; thus, adding water content to IMH does not significantly increase the explained variation of R2´.

IMH, intramyocardial hemorrhage

Figure legends

Figure 1. Study design

The study population comprised 20 pigs used to characterize intramyocardial hemorrhage during the first week after ischemia/ reperfusion by histological techniques and CMR imaging. § Tissue for IMH analysis was unavailable for one pig in the 120 min group, and CMR data for this animal was therefore excluded from the analysis.

CMR, cardiac magnetic resonance; H/E, hematoxylin-eosin; I/R, ischemia/reperfusion

Figure 2. CMR definition of intramyocardial hemorrhage

*Representative CMR scans during the first week after I/R injury. Images selected for the echo time (TE) 47 msec (T2) and 10 msec (T2*W).*

Figure 3. Histological definition of IMH and microvascular obstruction in different regions of same tissue sample

(A,B) Intramyocardial hemorrhage within the infarct core zone. (A) RBCs in the parenchyma are not confined to microvessels. (B) Microvascular density, assessed by anti-CD31 staining, is clearly diminished. (C,D) Representative example of microvascular obstruction. (C) RBCs are plugged inside a microvessel. (D) Anti CD31 staining confirms endothelial integrity.

H/E, hematoxylin-eosin.

Figure 4. Correlation between CMR relaxation times (T2* and R2*) and histological IMH

Results for correlations with all pigs (hemorrhagic and non-hemorrhagic) are plotted in Figure S4.

Figure 5. Correlation between CMR relaxation times (R2* and R2´) and histopathological findings (histological IMH and water content)

Results for correlations with all pigs (hemorrhagic and non-hemorrhagic) are plotted in Figure S5.

Fig 1

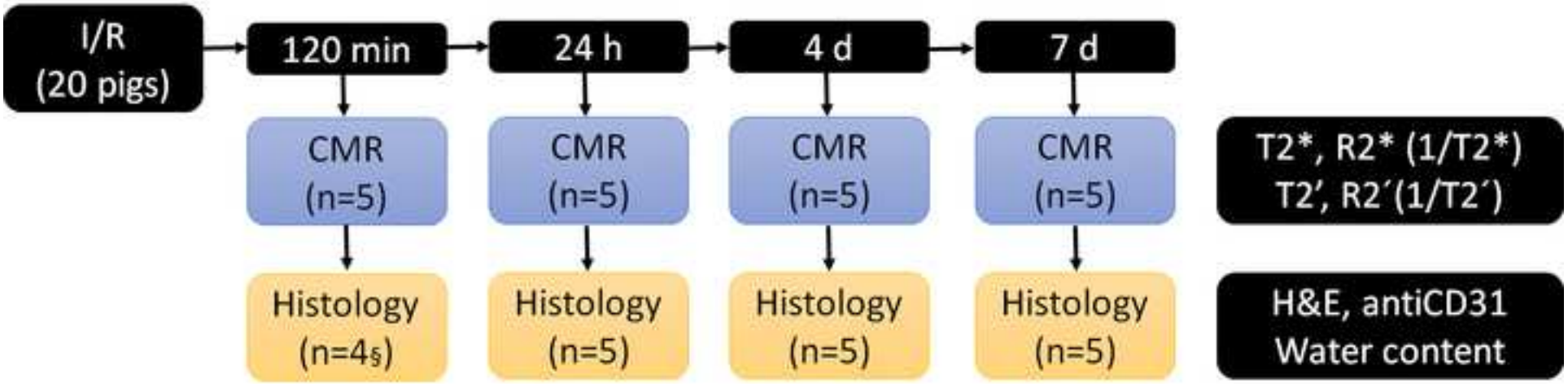
I/R
(20 pigs)
120 min
24 h
4 d
7 d
CMR
(n=5)
CMR
(n=5)
CMR
(n=5)
CMR
(n=5)
Histology
(n=4§)
Histology
(n=5)
Histology
(n=5)
Histology
(n=5)
T2*, R2* (1/T2*)
T2', R2´(1/T2´)
H&E, antiCD31
Water content

Fig 2

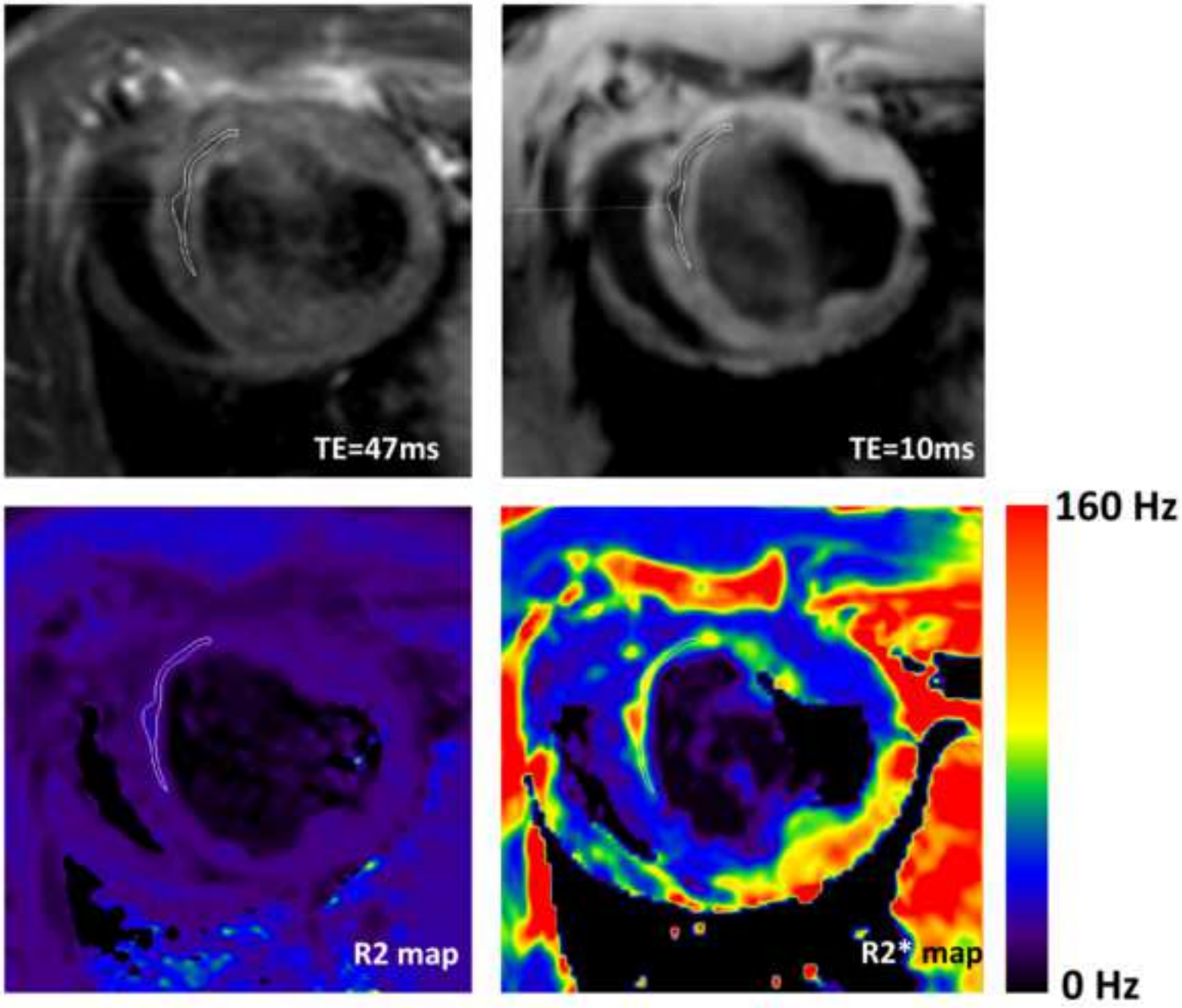

Fig 3

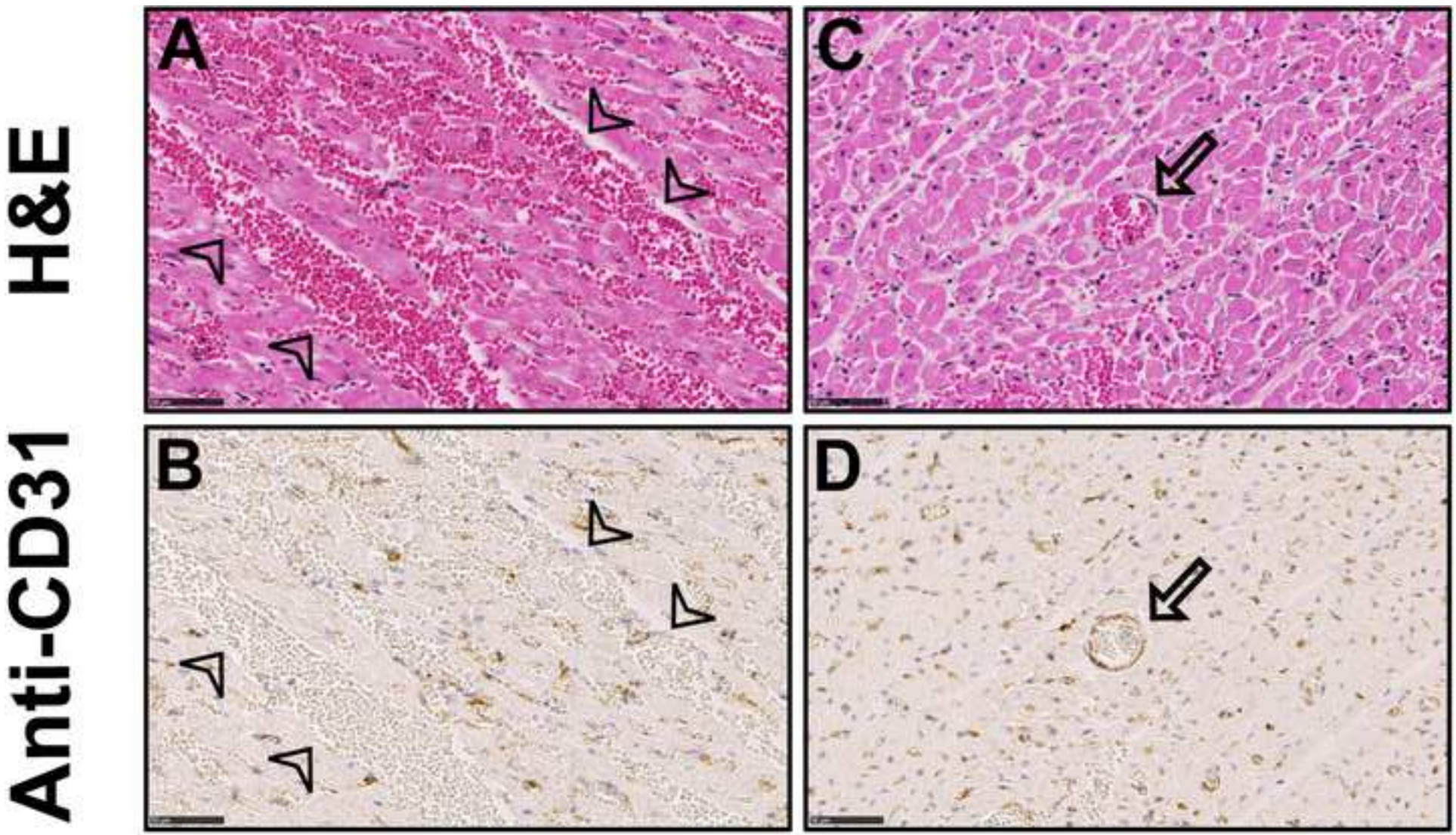

Fig 4

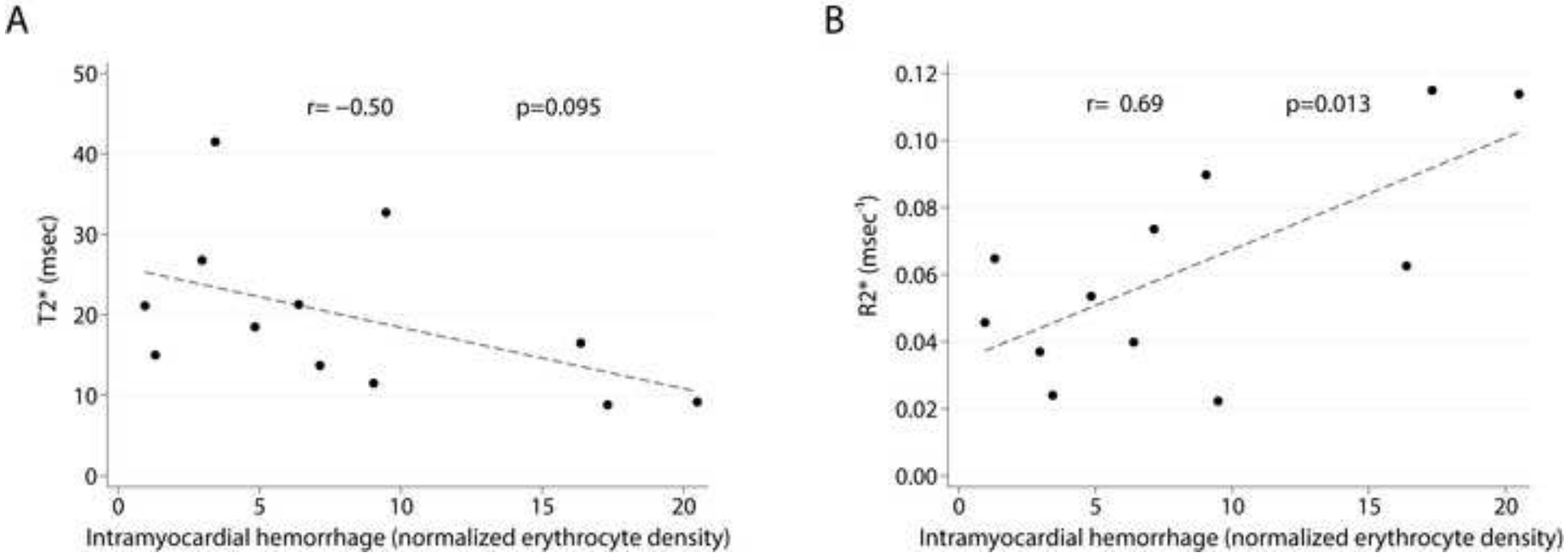
A
r= −0.50
p=0.095
T2* (msec)
50
40
30
20
10
0
0
5
10
15
20
Intramyocardial hemorrhage (normalized erythrocyte density)
B
r= 0.69
p=0.013
R2* (msec^{-1})
0.12
0.10
0.08
0.06
0.04
0.02
0.00
0
5
10
15
20
Intramyocardial hemorrhage (normalized erythrocyte density)

Fig 5

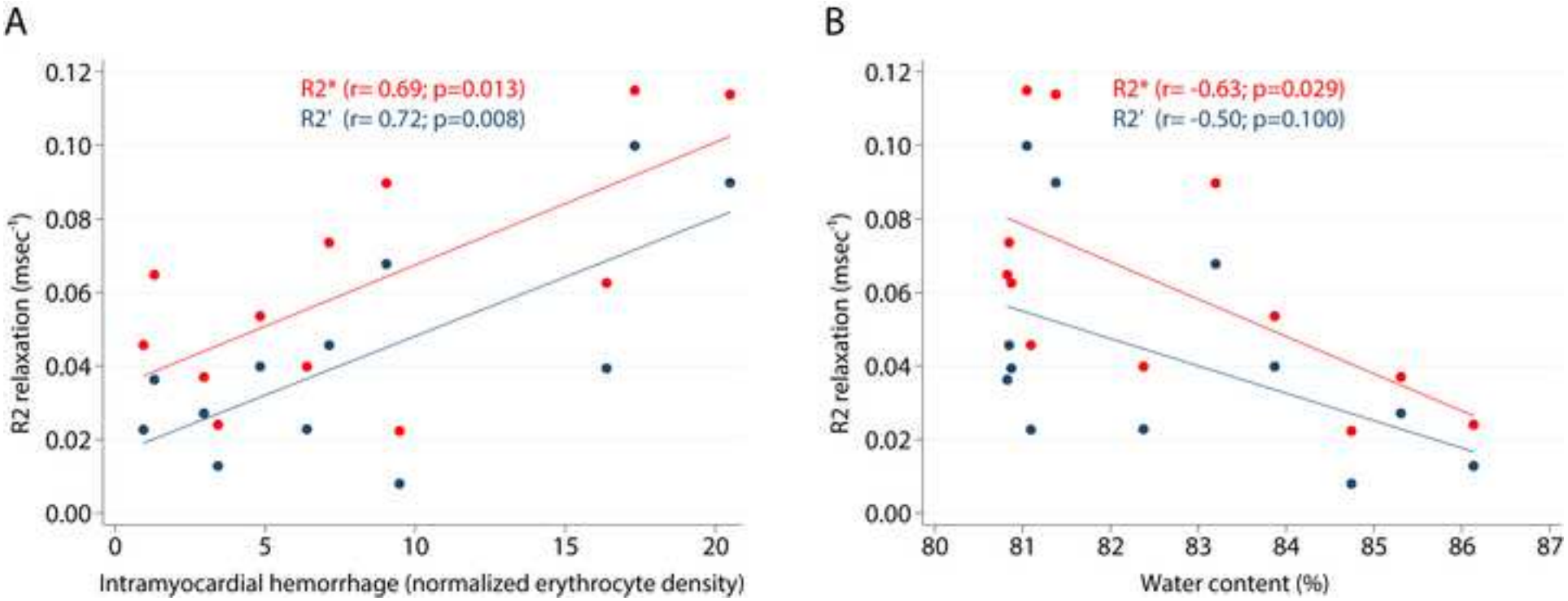
A
R2* (r= 0.69; p=0.013)
R2' (r= 0.72; p=0.008)
R2 relaxation (msec-1)
0.12
0.10
0.08
0.06
0.04
0.02
0.00
0
5
10
15
20
Intramyocardial hemorrhage (normalized erythrocyte density)
B
R2* (r= -0.63; p=0.029)
R2' (r= -0.50; p=0.100)
R2 relaxation (msec-1)
80
81
82
83
84
85
86
87
Water content (%)

Fig S1

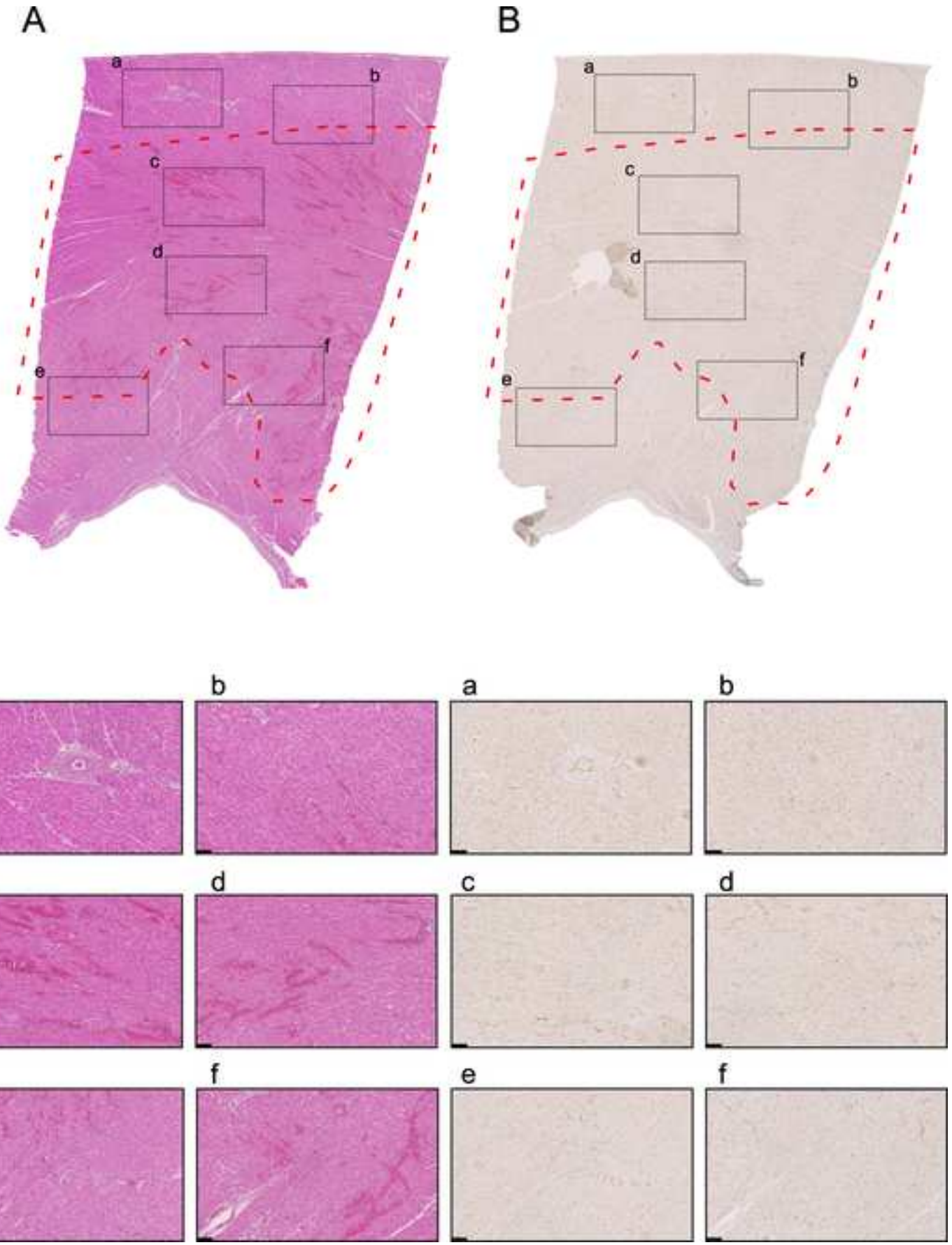

Fig S2

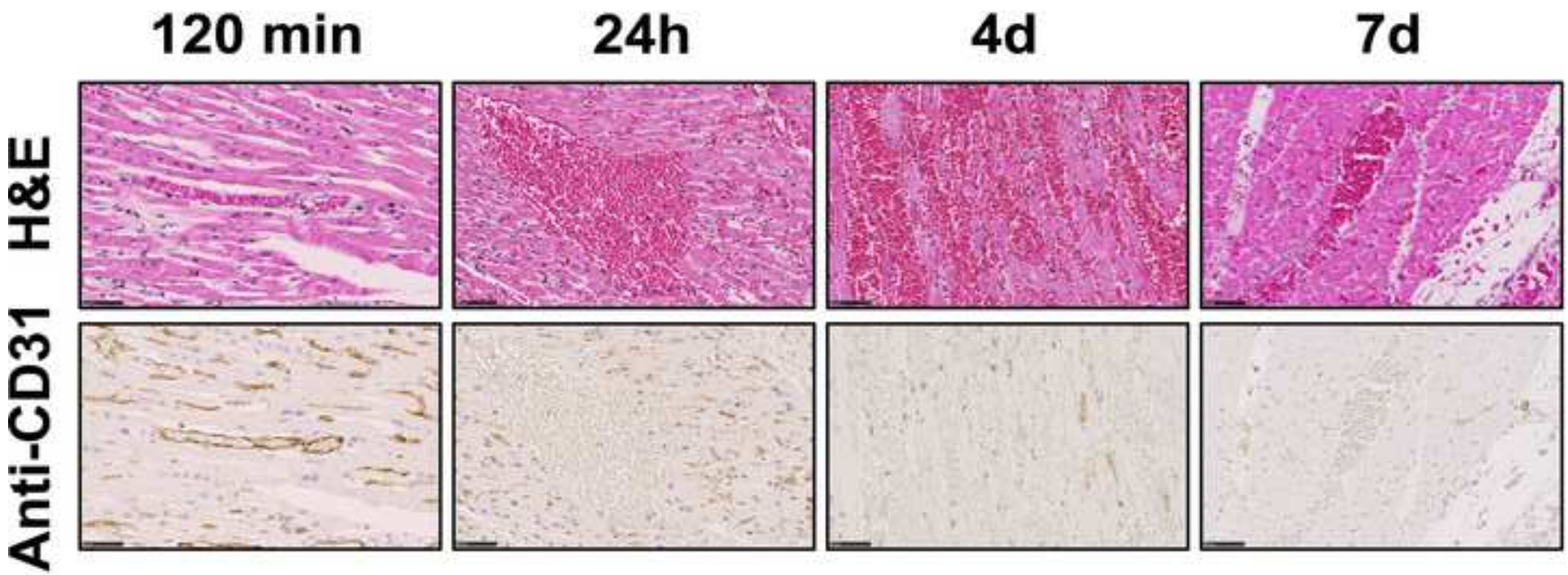

Fig S3

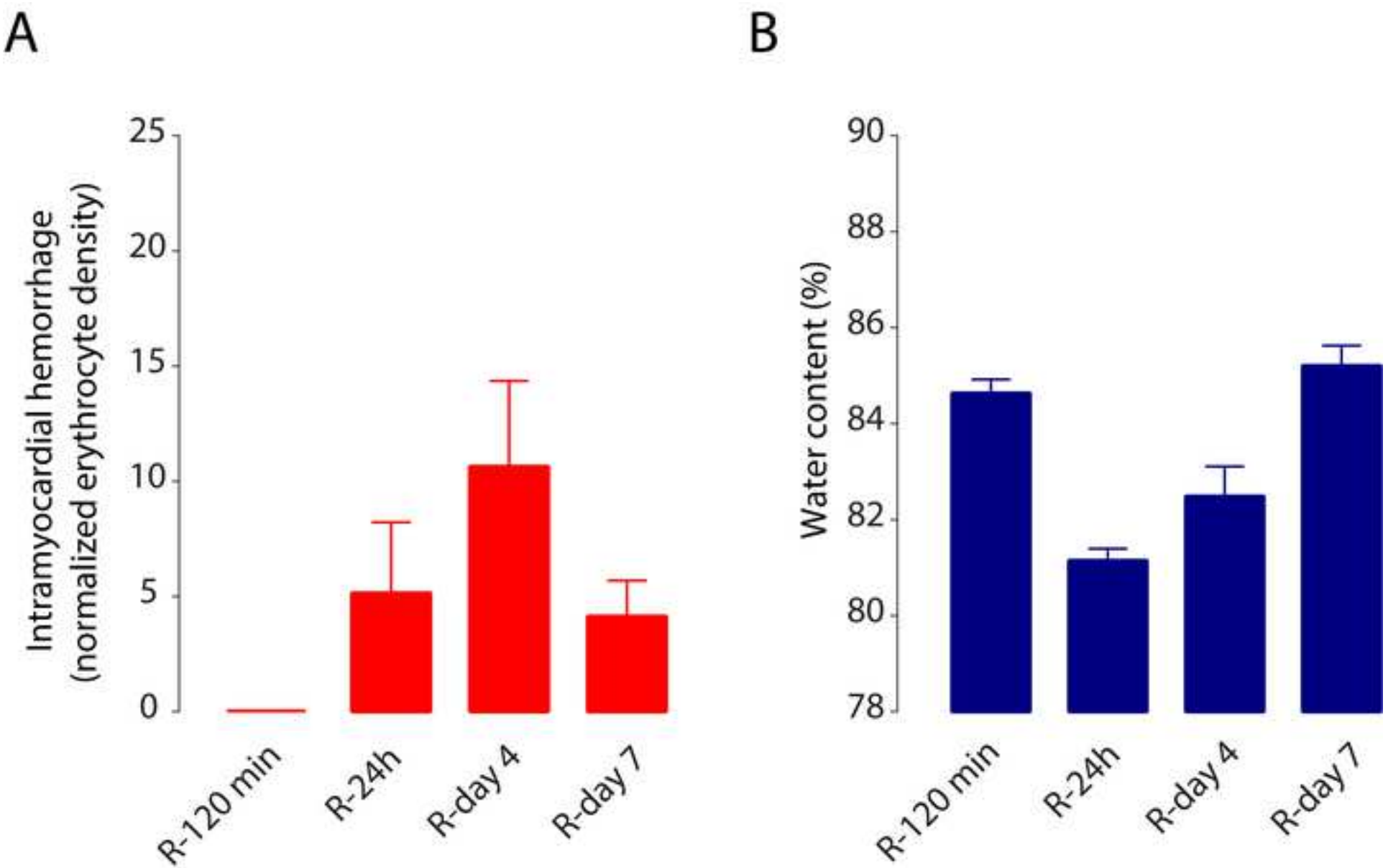
A
Intramyocardial hemorrhage
(normalized erythrocyte density)
25
20
15
10
5
0
R-120 min
R-24h
R-day 4
R-day 7
B
Water content (%)
90
88
86
84
82
80
78
R-120 min
R-24h
R-day 4
R-day 7

Fig S4

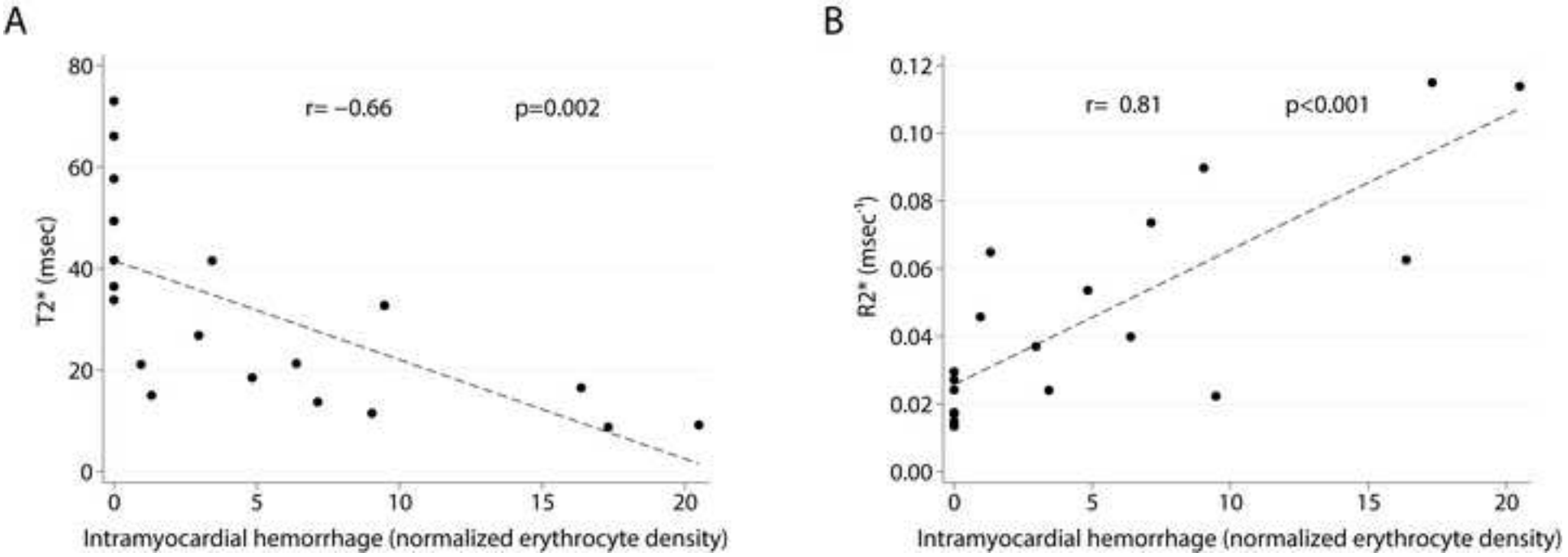
A
80
60
40
20
0
T2* (msec)
r= −0.66
p=0.002
0
5
10
15
20
Intramyocardial hemorrhage (normalized erythrocyte density)
B
0.12
0.10
0.08
0.06
0.04
0.02
0.00
R2* (msec-1)
r= 0.81
p<0.001
0
5
10
15
20
Intramyocardial hemorrhage (normalized erythrocyte density)

Fig S5

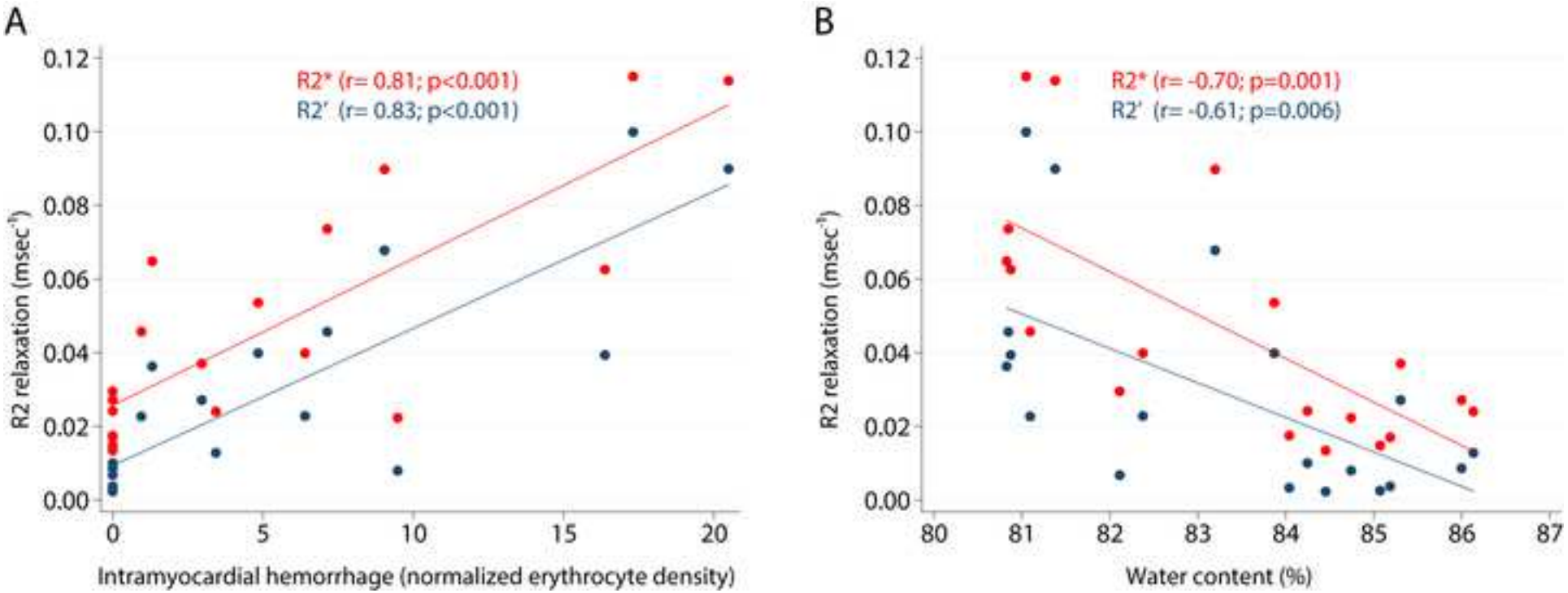
A
R2* (r= 0.81; p<0.001)
R2' (r= 0.83; p<0.001)
R2 relaxation (msec-1)
0.12
0.10
0.08
0.06
0.04
0.02
0.00
0
5
10
15
20
Intramyocardial hemorrhage (normalized erythrocyte density)
B
R2* (r= -0.70; p=0.001)
R2' (r= -0.61; p=0.006)
R2 relaxation (msec-1)
80
81
82
83
84
85
86
87
Water content (%)